

Regular Article - Experimental Physics

Proton branching ratios in ²²Mg for X-ray bursts

S. H. Kim¹, K. Y. Chae^{1,a}, D. W. Bardayan², J. C. Blackmon^{3,4}, K. A. Chipps^{4,5,6}, R. Hatarik^{7,8}, K. L. Jones⁶, M. J. Kim¹, R. L. Kozub⁹, J. F. Liang⁴, C. Matei^{10,11}, B. H. Moazen⁶, C. D. Nesaraja^{4,6}, P. D. O'Malley^{2,12}, S. D. Pain^{4,8}, M. S. Smith⁴

- ¹ Department of Physics, Sungkyunkwan University, Suwon 16419, Republic of Korea
- ² Department of Physics, University of Notre Dame, Notre Dame, IN 46556, USA
- ³ Department of Physics and Astronomy, Louisiana State University, Baton Rouge, LA 70803, USA
- ⁴ Physics Division, Oak Ridge National Laboratory, Oak Ridge, TN 37831, USA
- ⁵ Colorado School of Mines, Golden, CO 80401, USA
- ⁶ Department of Physics and Astronomy, University of Tennessee, Knoxville, TN 37996, USA
- ⁷ Lawrence Livermore National Laboratory, Livermore, CA 94550, USA
- ⁸ Department of Physics and Astronomy, Rutgers University, Piscataway, NJ 08854, USA
- ⁹ Department of Physics, Tennessee Technological University, Cookeville, TN 38505, USA
- 10 Extreme Light Infrastructure-Nuclear Physics (ELI-NP), Horia Hulubei National Institute for R&D in Physics and Nuclear Engineering (IFIN-HH), 077125 Buchurest-Magurele, Romania
- ¹¹ Oak Ridge Associated Univesities, Oak Ridge, TN 37831, USA
- ¹² Department of Physics and Astronomy, Rutgers University, New Brunswick, NJ 08903, USA

Received: 11 January 2023 / Accepted: 8 May 2023 / Published online: 23 May 2023 © The Author(s), under exclusive licence to Società Italiana di Fisica and Springer-Verlag GmbH Germany, part of Springer Nature 2023 Communicated by Maria Borge

Abstract Decay protons from ²²Mg energy levels populated through a previously reported ²⁴Mg(p, t)²²Mg transfer reaction (Chae et al. in Phys Rev C 79:055804, 2009) have been analyzed for proton branching ratios as a follow-up analysis. The measurement was performed at the Holifield Radioactive Ion Beam Facility of Oak Ridge National Laboratory by utilizing 41-MeV proton beams and ²⁴Mg solid targets. Decay protons and reaction tritons were simultaneously detected with a silicon detector array. By investigating the ²⁴Mg(p, t)²²Mg*(p)²¹Na channels, the proton branching ratios of five ²²Mg excited states were obtained. The measured branching ratios provide constraints on the proton partial widths of the populated ²²Mg levels, which have implications for X-ray burst nucleosynthesis.

1 Introduction

X-ray bursts (XRB) are some of the most interesting astrophysical phenomena, and occur in the atmosphere of an accreting neutron star in close binary star systems. [1] Heavy elements up to Cd-Sn can be synthesized during the burst within $\sim 10\,\mathrm{s}$ through thermonuclear reactions on protonrich unstable nuclei. Since thermonuclear reactions power XRBs, many nuclear parameters should be well studied to

Despite its importance, the 21 Na(p, γ) 22 Mg reaction rate at typical XRB temperatures is still controversial. The reaction rates reported by Cyburt et al. [5] and that by Iliadis et al. [6] differ by one order of magnitude. Cyburt et al. calculated the 21 Na(p, γ) 22 Mg reaction rate theoretically using the NON-SMOKER WEB code version 5.0w [7]. Iliadis et al. obtained the 21 Na(p, γ) 22 Mg reaction rate using a Monte-Carlo method with empirical resonance parameters mainly adopted from Refs. [8] and [9]. Therefore, more measurements are needed to better estimate the reaction rate at XRB temperatures.

Since the 21 Na(p, γ) 22 Mg reaction rate strongly depends on the properties of 22 Mg energy levels above the proton threshold at 5.504 MeV, many resonance parameters including the excitation energies, spins, parities and partial widths of the levels are required to estimate the reaction rate correctly. Although many parameters have been revealed through previous studies utilizing various nuclear reactions



understand XRB properties such as peak temperatures, luminosity, and isotopic abundances produced via nucleosynthesis. It is believed that the breakout from the hot CNO cycle can be provided through the 18 Ne(α , p) 21 Na reaction when the critical values of density and temperature are reached [2]. Then the 21 Na(p, γ) 22 Mg reaction can initiate the rapid proton capture process (rp-process) [3,4].

^a e-mail: kchae@skku.edu (corresponding author)

112 Page 2 of 8 Eur. Phys. J. A (2023) 59:112

[8–17], there are still remaining parameters yet to be determined.

The 24 Mg(p, t) 22 Mg transfer reaction was previously studied to clarify the level structure of 22 Mg especially above the α -threshold at 8.14 MeV [15], which enabled the astrophysical 18 Ne(α , p) 21 Na reaction rate to be updated accordingly. The angular distributions of the reaction tritons were extracted for seven 22 Mg energy levels. The empirical angular distributions were then compared with the Distorted Wave Born Approximation (DWBA) calculations to deduce the spins and parities of the energy levels by using computer code DWUCK5 [18]. In the present work, the proton decay channels of several 22 Mg levels populated from the 24 Mg(p, t) 22 Mg reaction are investigated as a follow-up analysis.

The experiment was performed at the Holifield Radioactive Ion Beam Facility (HRIBF) at Oak Ridge National Laboratory (ORNL) [19] using 41 MeV proton beams and ²⁴Mg foils. The thickness of isotopically-enriched (> 99.9%) ²⁴Mg target was approximately 500 µg/cm². The beam current was continuously monitored with a graphite beam stop located downstream of the target chamber. The recoiling particles were detected by the annular silicon detector array, SIDAR [20]. The SIDAR was composed of three trapezoidal wedges of 100- μ m-thick ΔE and 1000- μ m-thick E telescopes. Each detector was segmented into 16 strips. The light recoil particles were identified by standard energy loss techniques. As shown in Fig. 2 of Ref. [15], the tritons from the ²⁴Mg(p, t)²²Mg reaction were clearly identified without significant contamination from other charged particles. The SIDAR covered the angular range of $18^{\circ} \leq \theta_{lab} \leq 48^{\circ}$. The energy gain of each strip was calibrated using 5.8-MeV α particles from a ²⁴⁴Cm radioactive source. The triton energies were then internally calibrated by using the well-known ²²Mg levels at $E_x = 1.247$, 3.308, 4.402, and 6.045 MeV. A schematic diagram of the experimental setup is shown in Fig. 1.

2 Analysis

2.1 Coincidence between reaction tritons and decay protons

As demonstrated previously [21,22,24], proton branching ratios can be extracted serendipitously from existing reaction data by comparing the number of times a resonance was formed, via the reaction products, with the number of times it decayed, via coincident decay particles. In this analysis, the number of the tritons from the $^{24}{\rm Mg(p,t)^{22}Mg}$ reaction and that of the decay protons were needed. A typical PID plot obtained at $\theta_{lab}=37^{\circ}$ is shown in Fig. 2. The events falling in the red gate are identified as tritons. Only the low-energy protons (0.8 MeV < E $_p$ < 3.2 MeV) stopped in the ΔE detectors were analyzed for the present work, because the experimental setup such as the proton beam energy, detec-

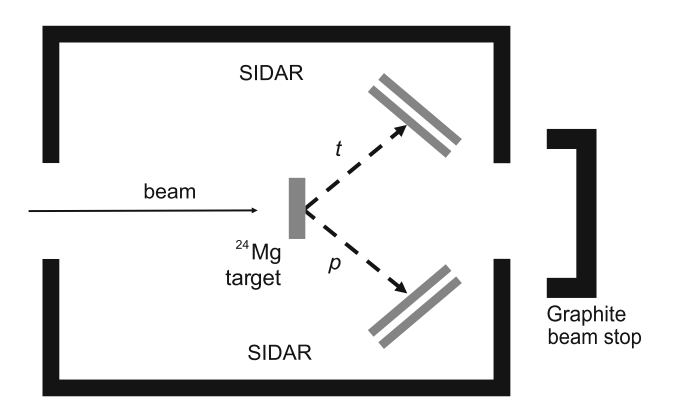


Fig. 1 A schematic diagram of the experimental setup

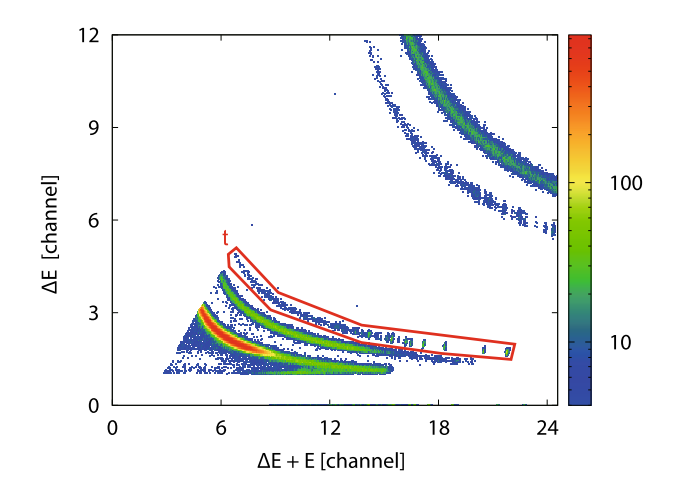


Fig. 2 Particle identification plot obtained at $\theta_{lab} = 37^{\circ}$. The red solid line is a gate for identifying the reaction tritons

tor thickness and detector threshold was optimized for the ²⁴Mg(p, t)²²Mg transfer reaction study.

By requiring a coincidence between the reaction tritons and the decay protons in the time window of 40 µs, the events from the proton decay of ²²Mg energy levels could be identified as shown in Fig. 3, which shows the two dimensional spectrum of proton energy (E_n) versus triton energy (E_t) . Two diagonal bands in the figure represent the events associated with ²⁴Mg(p, t)²²Mg*(p)²¹Na channels. The upper gate, labeled as p0, shows the decay events from the excited states of ²²Mg to the ground state of ²¹Na. Similarly, the events in the p1 gate are correlated to the decays to the first excited state of 21 Na (E_x = 0.332 MeV). The events appearing at rightbottom side, $E_t > 12.3$ MeV, seem to have clear structure in Figs. 3 and 5. However, they were not analyzed, since the discriminator threshold of several silicon strip detectors were rather high and therefore the protons at the energies relevant for the group were not recorded. The clusters at left-bottom side in the figure were identified as the decay events to the second excited state of 21 Na ($E_x = 1.716$ MeV) by constructing the ²¹Na excitation energy spectrum (Fig. 4). However,



Eur. Phys. J. A (2023) 59:112 Page 3 of 8 112

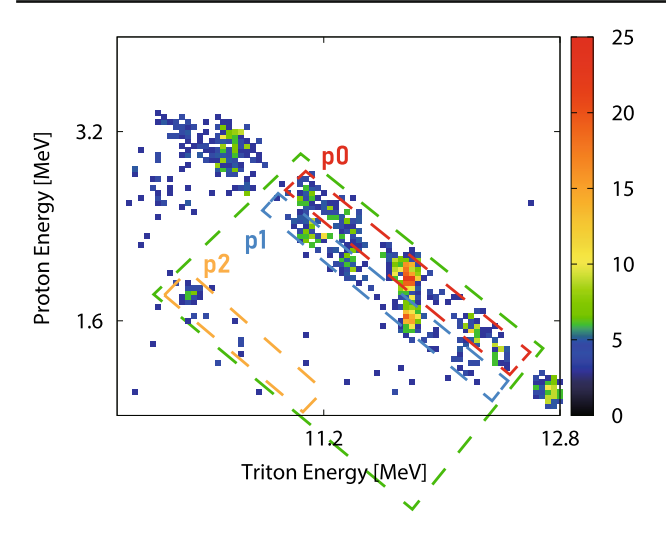


Fig. 3 Two-dimensional energy spectrum of the coincident proton energy (E_p) versus triton energy (E_t) . Diagonal gates labeled as p0 and p1 are drawn to analyze the corresponding decay channel. The p2 gate is also drawn but not analyzed because of insufficient statistics. The green gate is for constructing the ²¹Na excitation energy spectrum (see text)

they were also excluded in the present analysis because of insufficient statistics.

To see if the coincident events do originate from the proton decay of 22 Mg levels, the high energy protons (E $_p > 3.2$ MeV) that can be clearly identified from the particle identification plot were considered. Using the protons, the coincident events were plotted in similar way. The result shows that the diagonal bands in Fig. 3 are well extrapolated from those obtained using the high energy protons. Kinematics calculations show that other decay channels such as 24 Mg(p, 22 Mg*(d) 20 Na are not possible.

Due to the rather small excitation energy of the first excited state, two groups in the figure are not well separated. To estimate the uncertainty caused from this issue, the ²¹Na excitation energy spectrum was constructed. A large gate that includes the p0 and p1 gates was drawn as shown in Fig. 3 (green dashed line). Based on the relativistic 4-vector kinematics considerations of the particles participating in the reaction such as protons, tritons, ²⁴Mg, ²²Mg, and ²¹Na ions, the coincident events were projected into the ²¹Na excitation energy. For each event in the gate, the excitation energy of ²²Mg, E_{22mg}, can be obtained using

$$(E_{22mg} + m_{22mg})^2 = m_p^2 + m_{24mg}^2 + m_t^2$$

$$-2(m_p + T_p)(m_t + T_t)$$

$$+2(m_p + T_p)m_{24mg} - 2(m_t + T_t)m_{24mg}$$

$$+\sqrt{[(m_p + T_p)^2 - m_p^2][(m_t + T_t)^2 - m_t^2]} \cos \theta, \quad (1)$$

where T and m are the kinetic energy measured in the laboratory frame (in MeV) and the mass (in MeV/ c^2) of the

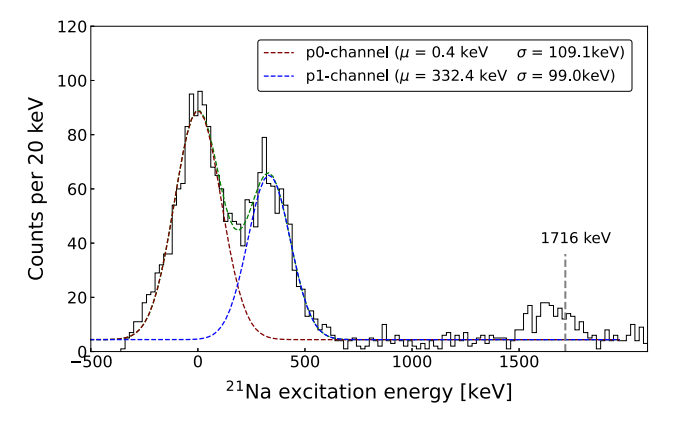


Fig. 4 The reconstructed 21 Na excitation energy spectrum from the decay events in the green gate shown in the Fig. 3. The values of the centroids μ and standard deviations σ are presented on the figure. The standard error means are 3.4 and 3.7 keV for the centroids of p0 and p1 channels, respectively. The peak near $E_x = 1.716$ MeV is from the decay events in the p2 gate of Fig. 3

corresponding particle, respectively. The excitation energy of 21 Na, E_{21Na} , is then expressed as

$$E_{21na} = E_{22mg} + m_{22mg} - T_p - m_p - m_{21na}.$$
 (2)

Using the equations above, the 21 Na excitation energy spectrum could be constructed as shown in the Fig. 4. The events were well fitted by Gaussian distributions. The difference between the values of the centroids was 0.333 ± 0.007 MeV, which agreed well with the energy difference between the ground state and the first excited state of 21 Na. Additionally, the decay events appearing at the left bottom side on the Fig. 3 are also plotted in the figure. The result shows that the reconstructed energies of the events appear near $E_x = 1.716$ MeV, which is the excitation energy of the second excited state of 21 Na. Therefore, it can be concluded that the events originated from the p2 channel. The uncertainties of the branching ratios caused by overlapping events were estimated to be about 5.0% for the p0 channel and 7.6% for the p1 channel.

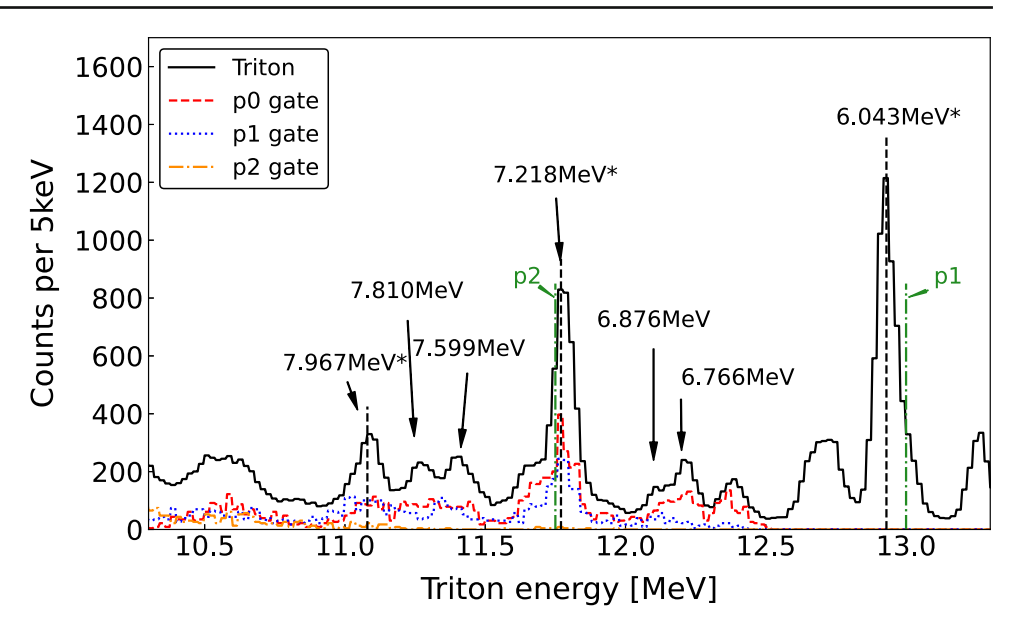
The triton energy spectra were reconstructed next as shown in Fig. 5. The red dashed line and blue dotted line represent the spectrum obtained from the p0-gated and p1-gated events, respectively. The black solid line is the triton single energy spectrum adopted from the ²⁴Mg(p, t)²²Mg study [15]. A total of 8 excited states in ²²Mg were identified above the proton-threshold with enough statistics.

The extracted values of excitation energies were internally calibrated using three well-known reference points: the energy levels at $E_x = 6.043$ MeV, 7.218 MeV, and 7.967 MeV. Not all identified levels were analyzed in the present work. For instance, the 7.967 and 7.356 MeV states are not considered, as they are suspected doublets [14,17]. Five excited states studied in the present work ($E_x = 6.766, 6.876, 7.218, 7.599$ and 7.810 MeV) and three reference points are labeled with their excitation energies in the figure.



112 Page 4 of 8 Eur. Phys. J. A (2023) 59:112

Fig. 5 The triton energy spectrum obtained at $\theta_{lab} = 33^{\circ}$ is shown as a black solid line. which is adopted from Ref. [15]. The identified levels and reference points are labeled with their excitation energies. The reference points are marked with an asterisk. The dashed vertical black lines represent the reference points used for the energy calibration. The spectra from the p0, p1 and p2 gate are corrected by the detection efficiency. The two vertical green lines represent the p1 and p2-threshold



Each spectrum in Fig. 5 was fitted assuming Gaussian distributions for populated levels with a constant background term. The peaks in the triton single spectrum were fitted first. Then, the corresponding peaks in the proton gated spectrum were fitted, using the same values of centroids and widths. The width of the peaks were fixed to be 40 keV for all considered peaks. From the fitting result, the background was estimated to be about 75 counts per 5 keV for triton single spectrum and 2 counts per 5 keV for proton gated spectra. One example for the $E_x = 7.599$ MeV level is shown in Fig. 6. Figure 6a–c show the results of the fittings for the triton single, p0 gated and p1 gated triton energy spectra, respectively.

By integrating each Gaussian function using fine tuned fitting parameters from (centroid)- (3σ) to (centroid)+ (3σ) , about 99.7% of the tritons and coincident protons could be reliably counted. From the ratio of the number of protons and that of tritons, the proton branching ratio of the 22 Mg excited state could be calculated. Because the solid angle covered by SIDAR was only about 6% of 4π and therefore not all protons from the decay of 22 Mg levels were detected, the total number of decay protons had to be corrected for the geometric detection efficiency. The solid angle covered by each strip of the SIDAR was obtained using a calibrated alpha emitting source, 244 Cm. The measured solid angle values agreed with geometric calculations within 3%. The result is summarized in Table 1.

2.2 Isotropic assumption

The branching ratio calculation in the previous section procedure described above is valid when the decay of protons is isotropic. To verify the validity of this assumption, a simple test was implemented. For each identified decay proton, the angle between a triton and the coincident proton pair

measured in the laboratory frame, θ_{lab} , was calculated by considering the geometry of SIDAR described in Sect. 1. The histograms of relative angles for the decay events from the 7.218 MeV state of 22 Mg to the ground and first excited state of 21 Na are shown as the black solid lines in Fig. 7. The statistical uncertainties are indicated as the error bars.

The experimental distribution was then compared with theoretical calculations. Calculated relative angle histograms obtained from the isotropic decay of protons in the center of mass frame are shown as blue-dashed lines. As shown in the figure, the isotropic decay lines well reproduce the experimental data regardless of the value of transferred angular momentum. Relative angle histograms for anisotropic decay are also shown in the figure as red-dotted lines. Unlike the previous proton branching ratio studies which used randomly biased cosine variations for anisotropic decay calculations [26–28], the calculated proton distributions were biased using the Legendre polynomials with proper angular transfer values in the present work. For instance, for the transition from the 7.218 MeV state ($J^{\pi} = 0^{+}$) to the ground state ($J^{\pi} = 0^{+}$) $3/2^+$), the Legendre Polynomial with l=2 $P_{l=2}(cos\theta)$ was assumed.

It is obvious from the figure that the isotropic decay assumption better reproduces the experimental result. Therefore, it is concluded that the proton decays are largely isotropic even when transferred angular momentum l is not 0. This conclusion is consistent with those from Refs. [26–28]. In order to account for any discrepancies between the anisotropic and isotropic decay, the systematic uncertainty is introduced, as previously done in Refs. [24–28]. In Ref. [24], for instance, the angular correlations between the heavy recoils and decay particles were calculated for proton decays with l = 0 to 3. The result shows that the uncertainties caused by the anisotropic decay assumption are from 5 to 30%



Eur. Phys. J. A (2023) 59:112 Page 5 of 8 112

Fig. 6 The fitted energy spectra of **a** triton single, **b** p0- and **c** p1-gated events for the $E_x = 7.599$ MeV level. The blue solid line is the sum of the constant term and the Gaussian distributions which are shown as the red dashed lines

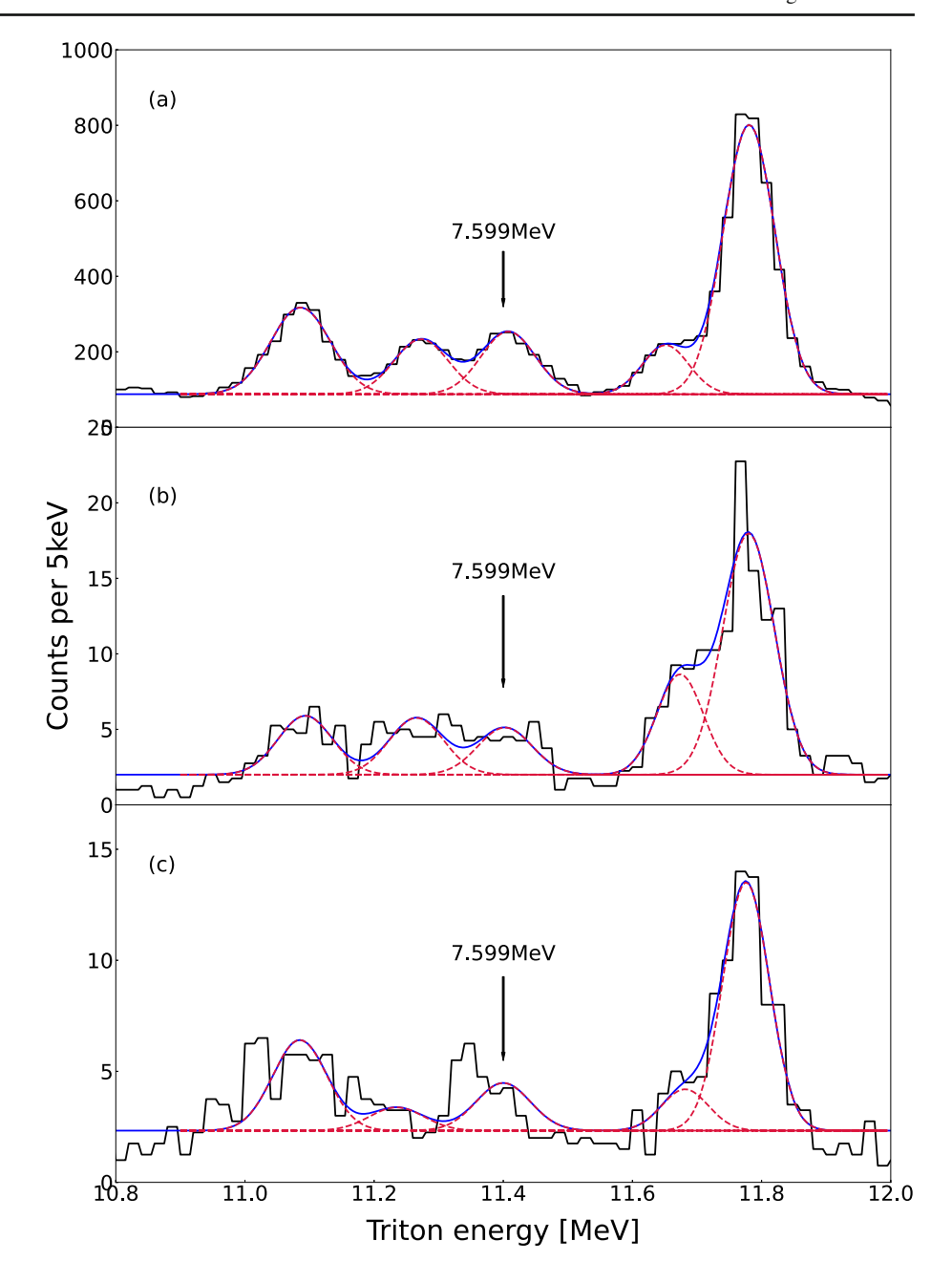


Table 1 The results of the branching ratio calculations. The excitation energies are taken from Ref. [23]. The value of B_{p1} is not computed for the states at $E_x = 6.766$ and 6.876 MeV because of the poor statistics in the p1-gated spectrum. The branching ratios are calculated assuming the isotropic decay of protons (See text). The total uncertainty includes the isotropic uncertainty and statistical uncertainty

$Sp_1 = 5.831$	E _x [MeV] [23]	B_{p0}	B_{p1}
	6.766 ± 0.012	0.54 ± 0.18	
	6.876 ± 0.012	0.81 ± 0.30	
$Sp_2 = 7.220$	7.218 ± 0.001	0.38 ± 0.12	0.24 ± 0.08
	7.599 ± 0.003	0.33 ± 0.12	0.23 ± 0.10
	7.810 ± 0.040	0.45 ± 0.16	0.13 ± 0.08

depending on the value of l=1 to 3 [24,25]. Therefore, a conservative systematic uncertainty of 30% is introduced in the present analysis.

3 Discussion

The 21 Na(p, γ) 22 Mg reaction rate can be expressed using the narrow-isolated resonance formalism [29]:



112 Page 6 of 8 Eur. Phys. J. A (2023) 59:112

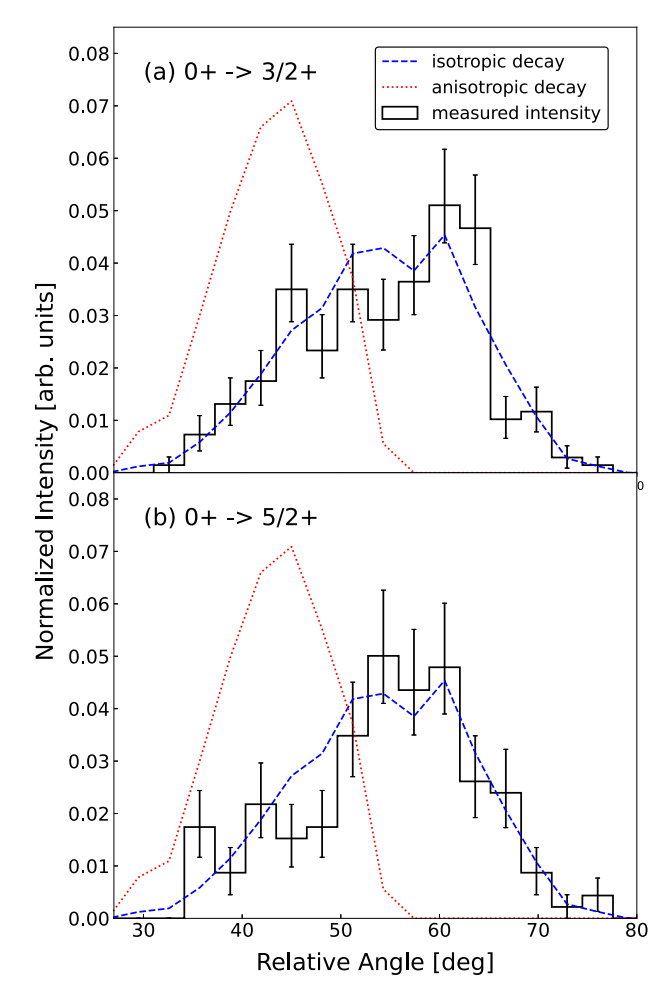


Fig. 7 The results of isotropic and anisotropic proton decay considerations for two transitions; from $J^{\pi} = 0^+$ ($E_x = 7.218$ MeV of 22 Mg) to **a** $J^{\pi} = 3/2^+$ (ground state of 21 Na) and **b** $J^{\pi} = 5/2^+$ (first excited state of 21 Na). The black solid lines represent the experimental distributions. The blue dashed lines and the red dotted lines are the results of the isotropic and anisotropic decay calculations, respectively. The error bars represent the statistical uncertainty of experimental distributions

$$N_A < \sigma v > = \frac{1.5399 \cdot 10^{11}}{(\mu T_9)^{3/2}} \times \sum_{i} (\omega \gamma)_i e^{-11.605E_i/T_9} \text{ cm}^3/\text{s/mol},$$
(3)

where i is the resonance index, E_i and $(\omega \gamma)_i$ are the resonance energy and strength in units of MeV, respectively, μ is the reduced mass of projectile and target nucleus in amu, and T_9 is the temperature in units of GK.

For a given resonance, the resonance strength $\omega\gamma$ is defined as

$$\omega \gamma \equiv \frac{2J+1}{(2J_p+1)(2J_{21Na}+1)} \frac{\Gamma_p \Gamma_{\gamma}}{\Gamma}, \tag{4}$$



where J, J_p , and J_{21Na} are the spins of the resonance, proton, and 21 Na, respectively. Γ , Γ_p and Γ_{γ} are the total width and partial widths of the compound nucleus, 22 Mg.

Since the proton decay branching ratio can be described as $\frac{\Gamma_p}{\Gamma}$ [13,24], the measured branching ratio values, B_{p0} and B_{p1} , give constraints on $\frac{\Gamma_{p0}}{\Gamma}$ and $\frac{\Gamma_{p1}}{\Gamma}$. However, to obtain precise values for the branching ratios, more information related to other open channels is still needed. For instance, the ²²Mg states at $E_x = 6.766$ and 6.876 MeV are open for the p0 and p1 decay channels. Only the p0 decay channel was observed in the present work.

The 21 Na(p, γ) 22 Mg reaction rate was calculated using the branching ratio values deduced from the present work. The resonance strength of

$$\omega \gamma_0 = \frac{2J+1}{(2J_p+1)(2J_{21Na}+1)} \frac{\Gamma_{p0}\Gamma_{\gamma}}{\Gamma}$$

$$= \frac{2J+1}{(2J_p+1)(2J_{21Na}+1)} B_{p0}\Gamma_{\gamma}$$
(5)

was used for the calculation. Considering the Gamow window for X-ray bursts, two 22 Mg levels studied in the present work (E_x = 6.766 and 6.876 MeV) were considered. The reaction Q-value of 5504.18 \pm 0.34 keV was adopted from Ref. [30].

The gamma width value of the 6.876 MeV level was deduced from the mirror state ($E_x = 7.051$ MeV in 22 Ne [14,17]), since no experimental data exists. Assuming that the reduced transition probability values $B(\omega L)$ are same for both states, the gamma width value of 4 ± 2 meV was obtained.

In the case of the 6.766 MeV state, the Γ_p value was measured twice in Refs. [9] and [16]. In Ref. [9], the reported values are $\Gamma_{p0} = 93.9 \pm 32.0 \text{ keV}$, $\Gamma_{p1} = 11.1 \pm 0.8 \text{ keV}$ and $\Gamma_{p0} + \Gamma_{p1} \approx \Gamma_{total} = 105.0 \pm 32.8$ keV. In Ref. [16], only the $\Gamma_p = \Gamma_{p0} + \Gamma_{p1}$ value was reported as 64 ± 20 keV. Since the Γ_p values from the references are discrepant, the Γ_{p0} value, and subsequently the $\Gamma_{total} = \frac{\Gamma_{p0}}{B_{p0}}$, could not be constrained reliably. Furthermore, the corresponding mirror state is not well defined. For instance, Matic et al. suggested that the E_x = 6.900 MeV level ($J^{\pi} = 0^{+}$) in ²²Ne is the mirror state [14]. However, the spin value of the level from other studies show discrepancies with this suggestion: $J^{\pi} = (1^+, 2^+)$ [16], 3 [11, 12], and 2^{-} [9, 17]. The mirror assignment of the 6.766 MeV level was not given in Ref. [17] Therefore, the gamma width of the level was assumed to be 1 ± 1 eV in the present work as previously done in Ref. [31] for the ¹⁹Ne level parameter estimations. The spin value is presumed to be 2^{-} [9,17]. The resonance parameters used in the reaction rate calculation are summarized in Table 2. Except for the 6.766 and 6.876 MeV levels, the parameters were taken from Ref. [6].

Eur. Phys. J. A (2023) 59:112 Page 7 of 8 112

Table 2 The resonance parameters used in the reaction rate calculation. The Q-value was taken from [30]. Parameters for the levels between $E_x = 5.711$ and 6.608 MeV are taken from Ref. [6]

E_x [MeV]	E_r [keV]	\mathbf{J}^{π}	ωγ [meV]
5.711	205.7 ± 0.5	2+	1.03 ± 0.21
5.954	454 ± 5	0+	0.86 ± 0.29
6.043	538 ± 13	0^{+}	11.5 ± 1.36
6.246	738.4 ± 1.0		219 ± 25
6.326	821.3 ± 0.9	1+	556 ± 77
6.608	1101.1 ± 2.5	2+	368 ± 62
6.766	1262 ± 12^a	2^{-b}	338 ± 343^{c}
6.876	1372 ± 1^{a}	1-	1.22 ± 0.89^{c}

^aCalculated with the corresponding excitation energies and the Q-value ^bTaken from Refs. [9,17]

The result of the reaction rate calculation is shown in the Fig. 8 as a red dashed line. The pink band in the figure represents the upper and lower limits of the reaction rate. The reaction rate reported in Ref. [6] is also shown as a black solid line for comparison. The upper and lower limits of the previous rate is represented by a gray shaded area. At the astrophysical temperatures (1 $< T_9 <$ 2), the new reaction rate is up to 2% higher than that of Ref. [6]. Notice that the present reaction rate calculated using the resonance strength expressed in Eq. 3 could be regarded as a lower limit, since only the p0 channel was considered. The most dominant uncertainty in the present rate originates from the uncertain gamma width for the 6.766 MeV level. Therefore, more precise measurements aiming to obtain the resonance parameters, especially the decay widths such as Γ_{γ} , and B_{p} are required in the future to obtain a better estimate of the 21 Na(p, γ) 22 Mg reaction rate.

4 Conclusion

By investigating the decay protons from ^{22}Mg states populated through the previously reported $^{24}\text{Mg}(p, t)^{22}\text{Mg}$ transfer reaction study [15], the proton decay branching ratios of several ^{22}Mg levels ($E_x = 6.766$, 6.876, 7.218, 7.599, and 7.810 MeV) were obtained. By requiring coincidences between the reaction tritons and decay protons, the two-dimensional energy spectrum of E_p versus E_t was obtained in this follow up analysis. The events from the $^{24}\text{Mg}(p, t)^{22}\text{Mg*}(p)^{21}\text{Na*}(E_x = 0.331\,\text{MeV})$ channel were identified. The triton energy spectra were constructed accordingly. From the triton energy spectrum, the energy levels of ^{22}Mg were identified. The yields of tritons and protons were obtained at each identified excited states. The yields of protons were

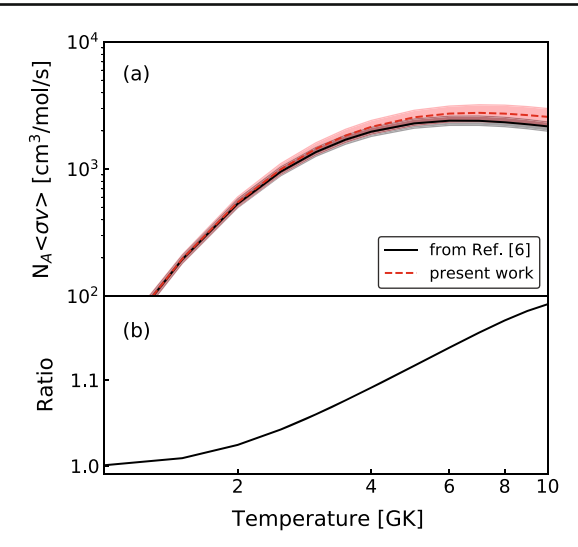


Fig. 8 The ²¹Na(p, γ)²²Mg reaction rate calculation result. The present result is compared with that of Ref. [6] in **a**. The pink and gray shading area represent the upper and lower limits of present rate and the reaction rate from Ref. [6], respectively. The ratio N_A < σv > $_{present}$ /N_A < σv > $_{Iliadis}$ is shown in **b**

corrected by considering the detection efficiency. The proton yields were then compared with that of the reaction tritons to obtain the proton branching ratios. The isotropic proton decay assumption was verified for the calculations. Using the branching ratio values for the 6.766 and 6.876 MeV levels obtained from the present work, the 21 Na(p, γ) 22 Mg reaction rate at XRB temperatures was calculated. The result shows that the new rate is slightly higher than the previous values reported in Ref. [6].

Acknowledgements This work was supported by the National Research Foundation of Korea (NRF) Grants funded by the Korea government (MSIT) (Grants no. 2016R1A5A1013277, and No. 2020R1A2C1005981). Additionally, the research was supported in part by the National Nuclear Security Administration under the Stewardship Science Academic Alliances program through the U.S. DOE Cooperative Agreement No. DE-FG52-08NA28552 with Rutgers University and Oak Ridge Associated Universities. This work was also supported in part by the Office of Nuclear Physics, Office of Science of the U.S. DOE under Contract No. DE-FG02-96ER40955 with Tennessee Technological University, Contract No. DE-FG02-96ER40983 with the University of Tennessee, and Contract No. DE-AC-05-00OR22725 with Oak Ridge National Laboratory; by the National Science Foundation under Contract No. PHY-2011890 with the University of Notre Dame and Contract No. PHY-1812316 with Rutgers University.

Data Availability Statement This manuscript has no associated data or the data will not be deposited. [Authors' comment: Data is available upon request from the authors.]

References

- J.L. Fisker, F.K. Thielemann, M. Wiescher, Astrophys. J. 608(1), L61 (2004)
- M. Wiescher, J. Görres, H. Schatz, J. Phys. G Nucl. Part. Phys. 25(6), R133–R161 (1999)



^cCalculated with the gamma width and the branching ratio values deduced in the present work

112 Page 8 of 8 Eur. Phys. J. A (2023) 59:112

- 3. H. Schatz, K. Rehm, Nucl. Phys. A 777, 601–622 (2006)
- 4. J.L. Fisker, H. Schatz, F.K. Thielemann, Astrophys. J. Suppl. Ser. **174**(1), 261 (2008)
- 5. R.H. Cyburt et al., Astrophys. J. Suppl. Ser. **189**(1), 240 (2010)
- C. Iliadis, R. Longland, A. Champagne, A. Coc, R. Fitzgerald, Nucl. Phys. A 841(1), 31 (2010)
- 7. T. Rauscher, Online code NON-SMOKER^{WEB}, version 5.0w and higher. https://nucastro.org/websmoker.html
- 8. J.M. D'Auria et al., Phys. Rev. C 69, 065803 (2004)
- 9. C. Ruiz et al., Phys. Rev. C 71, 025802 (2005)
- 10. R.A. Paddock, Phys. Rev. C 5, 485 (1972)
- A.A. Chen, R. Lewis, K.B. Swartz, D.W. Visser, P.D. Parker, Phys. Rev. C 63, 065807 (2001)
- J.A. Caggiano, W. Bradfield-Smith, J.P. Greene, R. Lewis, P.D. Parker, K.E. Rehm, D.W. Visser, Phys. Rev. C 66, 015804 (2002)
- 13. B. Davids et al., Phys. Rev. C 68, 055805 (2003)
- 14. A. Matic et al., Phys. Rev. C 80, 055804 (2009)
- 15. K.Y. Chae et al., Phys. Rev. C 79, 055804 (2009)
- 16. J.J. He et al., Phys. Rev. C 80, 015801 (2009)
- 17. L.Y. Zhang et al., Phys. Rev. C 89, 015804 (2014)
- 18. P.D. Kunz, http://spot.colorado.edu/kunz/DWBA.html
- 19. J.R. Beene et al., AIP Conf. Proc. 1336(1), 576 (2011)
- 20. D.W. Bardayan et al., Phys. Rev. C 63, 065802 (2001)

- 21. B. Davids et al., Phys. Rev. C 67, 012801 (2003)
- 22. S. Utku et al., Phys. Rev. C 57, 2731 (1998)
- 23. M.S. Basunia, Nucl. Data Sheets 127, 69 (2015)
- 24. K.A. Chipps et al., Phys. Rev. C 82, 045803 (2010)
- 25. K.A. Chipps et al., Phys. Rev. C 86, 014329 (2012)
- 26. K.A. Chipps et al., Phys. Rev. C 95, 044319 (2017)
- 27. M.J. Kim et al., Phys. Rev. C 104, 014323 (2021)
- 28. C.H. Kim et al., Phys. Rev. C 105, 025801 (2022)
- C. Iliadis, Nuclear Physics of Stars, 2nd edn. (Wiley-VCH, Weinheim, 2015), p.183
- 30. M. Mukherjee et al., Phys. Rev. Lett. 93, 150801 (2004)
- C.D. Nesaraja, N. Shu, D.W. Bardayan, J.C. Blackmon, Y.S. Chen,
 R.L. Kozub, M.S. Smith, Phys. Rev. C 75, 055809 (2007)

Springer Nature or its licensor (e.g. a society or other partner) holds exclusive rights to this article under a publishing agreement with the author(s) or other rightsholder(s); author self-archiving of the accepted manuscript version of this article is solely governed by the terms of such publishing agreement and applicable law.

